Nephrol Dial Transplant (2019) 34: 947–960
doi: 10.1093/ndt/gfy282
Advance Access publication 21 September 2018

Protein kinase C beta deficiency increases glucose-mediated peritoneal damage via M1 macrophage polarization and up-regulation of mesothelial protein kinase C alpha

Michael S. Balzer[1], Alexandra Helmke[1], Martina Ackermann[1,2], Janis Casper[1], Lei Dong[1], Marcus Hiss[1], Yulia Kiyan[1], Song Rong[1], Kai Timrott[3], Sibylle von Vietinghoff[1], Le Wang[1,4], Hermann Haller[1] and Nelli Shushakova[1,2]

[1]Department of Nephrology and Hypertension, Hannover Medical School, Hannover, Germany, [2]Phenos, Hannover, Germany, [3]Department for General, Abdominal and Transplant Surgery, Hannover Medical School, Hannover, Germany, and [4]Department of Nephrology, Tongji Medical College, Wuhan, China

Correspondence and offprint requests to: Michael S. Balzer, E-mail: balzer.michael@mh-hannover.de
Nelli Shushakova, E-mail: nshushakova@phenos.com;

ABSTRACT

Background. Peritoneal membrane (PM) damage during peritoneal dialysis (PD) is mediated largely by high glucose (HG)–induced pro-inflammatory and neo-angiogenic processes, resulting in PM fibrosis and ultrafiltration failure. We recently demonstrated a crucial role for protein kinase C (PKC) isoform α in mesothelial cells.

Methods. In this study we investigate the role of PKCβ in PM damage *in vitro* using primary mouse peritoneal macrophages (MPMΦ), human macrophages (HMΦ) and immortalized mouse peritoneal mesothelial cells (MPMCs), as well as *in vivo* using a chronic PD mouse model.

Results. We demonstrate that PKCβ is the predominant classical PKC isoform expressed in primary MPMΦ and its expression is up-regulated *in vitro* under HG conditions. After *in vitro* lipopolysaccharides stimulation $PKC\beta^{-/-}$ MPMΦ demonstrates increased levels of interleukin 6 (IL-6), tumour necrosis factor α, and monocyte chemoattractant protein-1 and drastically decrease IL-10 release compared with wild-type (WT) cells. *In vivo*, catheter-delivered treatment with HG PD fluid for 5 weeks induces PKCβ up-regulation in omentum of WT mice and results in inflammatory response and PM damage characterized by fibrosis and neo-angiogenesis. In comparison to WT mice, all pathological changes are strongly aggravated in $PKC\beta^{-/-}$ animals. Underlying molecular mechanisms involve a pro-inflammatory M1 polarization shift of MPMΦ and up-regulation of PKCα in MPMCs of $PKC\beta^{-/-}$ mice. Finally, we demonstrate PKCβ involvement in HG-induced polarization processes in HMΦ.

Conclusions. PKCβ as the dominant PKC isoform in MPMΦ is up-regulated by HG PD fluid and exerts anti-inflammatory effects during PD through regulation of MPMΦ M1/M2 polarization and control of the dominant mesothelial PKC isoform α.

Keywords: fibrosis, inflammation, macrophage polarization, peritoneal dialysis, protein kinase C

INTRODUCTION

Peritoneal dialysis (PD) is a renal replacement therapy that relies on the peritoneal membrane (PM) as a dialyzer providing adequate solute and water transport when osmotically challenged by glucose-containing PD fluid (PDF) solutions. Although equivalent to haemodialysis with respect to adequacy, mortality and other outcome parameters [1, 2], the most important challenge in PD therapy is long-term PM preservation, as the glucotoxic environment triggers inflammation, angiogenesis and fibrosis [3]. These pathological processes can ultimately lead to detrimental functional alterations [4] necessitating a change in renal replacement therapy. PM pathophysiology within the glucotoxic milieu of PD treatment is complex and still inadequately understood [5]. Thus studies identifying potential interventional targets are desperately needed in order to facilitate longer PD half-lives for patients.

The protein kinase C (PKC) superfamily consists of classical (α, βI, βII, γ), novel (δ, ϵ, θ, η) and atypical (ζ, λ/ι) isoforms. Expression patterns of different PKC isoforms are tissue and cell specific. Whereas some of them, such as PKCα, βI, βII, ϵ, δ, and ζ, are nearly ubiquitously expressed, the expression of others, such as PKCγ, η and θ, is restricted to specific cell types [6]. Multiple PKC isozymes can be present in the same cell, and depending on the stimulus, they translocate to different

subcellular compartments such as the plasma membrane, tight junctions, the Golgi apparatus and the endoplasmic reticulum, mediating differential signaling responses [6, 7].

Abundant evidence from the literature shows that PKCβ signal transduction mediates glucotoxic effects in various organ systems, including myocardial ischaemia/reperfusion injury [8], endothelial dysfunction and diabetic atherosclerosis [9], oxidative stress [10], vascular inflammation [11], insulin resistance [12] and diabetic nephropathy [13]. We have previously shown in a chronic high-glucose (HG) PD animal model that PKCα expression in mouse peritoneal mesothelial cells (MPMCs) plays a crucial role in PM pathophysiology mediating inflammatory, neo-angiogenic and fibrotic response [14]. Although the expression of PKCβ in MPMCs is very low, another cell type expressing PKCβ, namely resident murine peritoneal macrophages (MPMΦ), contributes significantly to PM damage during PD [15]. Recent studies have demonstrated that MPMΦ relies on PKC in order to fine-tune inflammation-controlling cytokine responses [16] and HG environment alters their phenotype and function [17].

We therefore aimed to investigate the possible role of PKCβ in PM damage *in vitro* using primary wild-type (WT) and $PKC\beta^{-/-}$ MPMΦ and immortalized WT, $PKC\alpha^{-/-}$, and $PKC\beta^{-/-}$ MPMCs as well as *in vivo* using experimental PD in $PKC\beta^{-/-}$ mice compared with WT controls.

MATERIALS AND METHODS

PD mouse model and modified ultrafiltration test

All experiments involving animals were approved by the Lower Saxony State Departments for Food Safety and Animal Welfare (#04-12/0847). Twelve-week-old female WT and $PKC\beta^{-/-}$ mice (129/Sv background) were treated daily for 5 weeks with either normal saline (0.9%, isotonic) (control) or with conventional PDF containing 4.25% glucose (CAPD/DPCA3, Fresenius, Bad Homburg, Germany) via a subcutaneously implanted mini-access port (Access Technologies, Skokie, IL, USA) as previously described [14]. Groups comprised 6 animals for saline and 12 for PDF treatment. On the last day of experimentation, a modified ultrafiltration test was performed to evaluate PM function (see Supplementary data). Thereafter, tissue samples were collected from the anterior abdominal wall for histologic analysis.

Flow cytometry and enzyme-linked immunosorbent assay (ELISA) measurements in peritoneal effluents

Inflammatory cell populations in peritoneal effluents were analysed by flow cytometry using a fluorescence-activated cell sorter (FACS) Canto II cytometer (BD Biosciences, Heidelberg, Germany). Monoclonal antibodies (BioLegend, San Diego, CA, USA) used to detect myeloid cells, macrophages, T cells and B cells are listed in the Supplementary data. Analyses were performed using FlowJo software (Tree Star, Ashland, OR, USA). Inflammatory cytokines interleukin 6 (IL-6), IL-10, IL-12, IL-17, interferon γ (IFN-γ), tumor necrosis factor α (TNF-α) and monocyte chemoattractant protein-1 (MCP-1) were analysed by bead-based flow cytometry assay (CBA kit, BD Biosciences), transforming growth factor β (TGF-β), vascular endothelial growth factor (VEGF) and macrophage inflammatory protein-2 (MIP-2) with a specific ELISA (R&D Systems, Wiesbaden, Germany) according to the manufacturer's instructions.

Morphologic and immunofluorescence analysis of peritoneum

The submesothelial layer thickness of the peritoneum was determined on 2.5-μm paraffin-embedded tissue sections stained with Masson's trichrome (Sigma-Aldrich, Munich, Germany) by blinded microscopy analysis (DM-IL microscope, DC300F camera, IM500 software; all Leica Microsystems, Wetzlar, Germany). Analyses are expressed as the mean of 40 independent measurements per animal at standardized interspaced locations on the peritoneum. Collagen I and III positivity was analysed on sections stained with picrosirius red (Sigma-Aldrich) using an integrated intensity thresholding method detailed in the Supplementary data (ImageJ software, National Institutes of Health, Bethesda, MD, USA); results are given as a percentage of the total tissue area.

Peritoneum was stained for CD31, F4/80, Gr1, CD4, CD8, MHCII, CD38, Arg-1 and PKCα (Supplementary data). PKCα staining was also performed in human peritoneal biopsies taken from PD patients and non-uraemic control patients undergoing surgery because of non-renal causes (excluding trauma, intra-abdominal neoplasia or inflammation) after informed consent according to the Declaration of Helsinki and local ethics board approval (MHH 2014/6715).

Stimulation of primary MPMΦ, transfection and subsequent stimulation of peripheral blood mononuclear cell (PBMC)-derived human macrophages

Resident MPMΦ were obtained from untreated mice by peritoneal lavage and cultivated as described previously [18]. MPMΦ were starved overnight in 1% FCS/RPMI 1640 medium prior to incubation with different glucose concentrations. In some experiments, MPMΦ were stimulated with 100 ng/mL lipopolysaccharides (LPS) (O111:B4, Sigma-Aldrich) for 7 h followed by RNA and protein analysis. Inflammatory cytokines were analysed in conditioned medium by flow cytometry and ELISA as described for peritoneal effluents.

PBMC-derived human macrophages (HMΦ) were generated from human peripheral blood cells obtained after informed consent and local ethics board approval (MHH 2010/807) as described previously [19]. In short, PBMCs were isolated by density gradient centrifugation (Biocoll 1.077, Biochrom, Berlin, Germany) and adherent cells were cultivated in 10% FCS/RPMI 1640 medium for 7 days until further experimentation. Gene transcription of PKCβ was inhibited in HMΦ with PKCβ-specific small interfering RNA (siRNA; sc-36255, Santa Cruz Biotechnology, Dallas, TX, USA) using JetPRIME transfection agent (Polyplus, Illkirch, France) in the presence of serum-containing medium as described by the manufacturer. As a control, scrambled siRNA was used (sc-37007, Santa Cruz Biotechnology). Successful knockdown was ensured using real-time quantitative polymerase chain reaction (PCR) and western blot. Post-transfection HMΦ were incubated in 1% FCS/RPMI

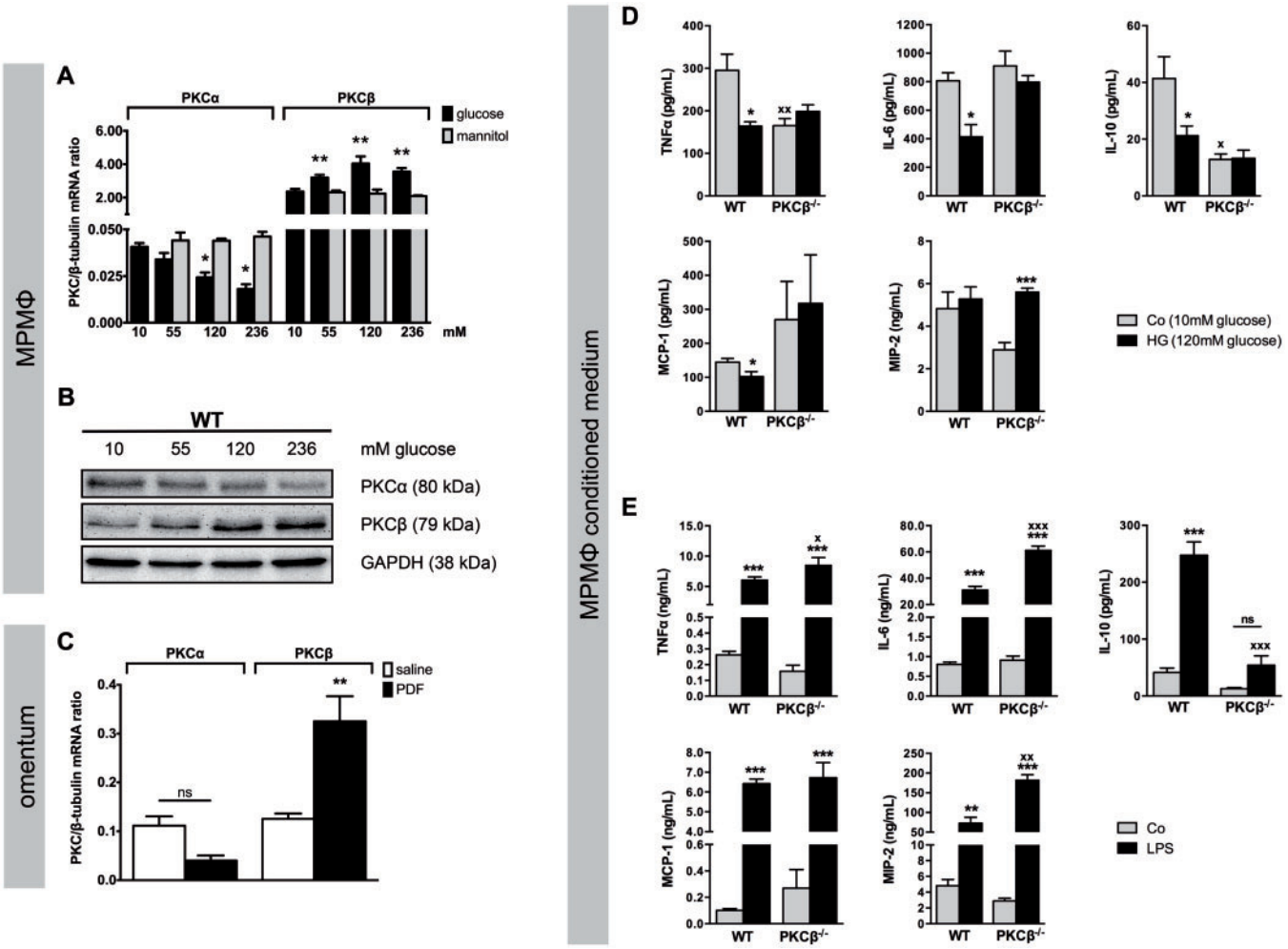

FIGURE 1: PKCβ is the predominant PKC isoform in MPMΦ, it is up-regulated by glucose *in vitro* and *in vivo* and its presence is necessary for mounting anti-inflammatory responses in an HG environment. (**A**) Real-time PCR of PKC isoforms α and β in primary MPMΦ treated with different glucose concentrations. Mannitol was used as an osmolar control. While PKCβ is up-regulated, PKCα is down-regulated by glucose in a dose-dependent manner [*$P < 0.05$ and **$P < 0.01$ versus respective control (10mM glucose) group]. (**B**) Western blot analysis of WT MPMΦ lysates demonstrates a similar glucose-dependent regulation of PKC isoform expression on the protein level. Glyceraldehyde-3-phosphate dehydrogenase was used as loading control. (**C**) Real-time PCR of PKC isoforms α and β in omentum of WT animals treated for 5 weeks with HG (4.25%) PDF and saline, respectively, demonstrates PDF-mediated induction of PKCβ. Beta-tubulin was used as a reference ($n = 6$ mice/group; **$P < 0.01$ versus respective saline group). (**D**) Concentrations of TNF-α, IL-6, IL-10, MCP-1 and MIP-2 in conditioned media from WT and *PKCβ*$^{-/-}$ MPMΦ under control (Co) conditions with NG (10 mM) or HG (120 mM) conditions. Compared with WT MPMΦ, *PKCβ*$^{-/-}$ cells lack HG-mediated regulation of pro- and anti-inflammatory mediators (*$P < 0.05$ and ***$P < 0.001$ versus respective control group; $^{x}P < 0.05$ and $^{xx}P < 0.01$ versus respective WT group). (**E**) Analysis similar to (D) after LPS stimulation. PKCβ deficiency exacerbates pro-inflammatory and disrupts anti-inflammatory mediator release (**$P < 0.01$ and ***$P < 0.001$ versus respective control group; $^{x}P < 0.05$, $^{xx}P < 0.01$ and $^{xxx}P < 0.001$ versus respective WT group).

1640 medium containing either normal glucose (NG, 10 mM) or high glucose (HG, 120 mM) concentrations for 48 h before analysis. Some cells were additionally stimulated with 100 ng/mL LPS in the last 14 h. Antibodies for flow cytometry are listed in the Supplementary data.

Stimulation of immortalized MPMCs with PDF and LPS

Immortalized MPMCs were generated and cultivated as described previously [14] and grown to 80% confluence. Cells were starved overnight in serum-free medium and then stimulated for 24 h with medium containing HG (120 mM) or NG (10 mM). PKCα activity was inhibited by pre-incubation of cells for 1 h with 5 μM Gö6976 (Calbiochem, Darmstadt, Germany), a cell-permeable reversible adenosine triphosphate–competitive PKCα/β inhibitor. MCP-1 in supernatants was analysed by flow cytometry as described for peritoneal effluents.

In another set of experiments, MPMCs were grown and starved similarly and then stimulated for 24 or 72 h with or without 100 ng/mL LPS. Inflammatory cytokines MCP-1, IL-6 and MIP-2 were analysed in conditioned medium by flow cytometry and ELISA.

Further experiments, which included pharmacological inhibition of PKCβ by isoform-specific inhibitor Ly333531 (ruboxistaurin), are detailed in the Supplementary data.

Western blotting, RNA extraction and real-time quantitative PCR

Cell lysate proteins were analysed for expression of PKCα and β by standard western blot analysis (Supplementary data).

Total RNA was extracted from omentum, MPMΦ, HMΦ and MPMCs using the RNeasy mini kit (Qiagen, Venlo, The Netherlands). TaqMan analysis was performed on a LightCycler 480 real-time PCR system using LightCycler 480 RNA Master Hydrolysis probes (Roche Applied Sciences, Penzberg, Germany); murine β-tubulin or human β-actin messenger RNA (mRNA) was measured as an internal standard. Primer sequences are available on request. Quantification was conducted using QGene software.

Statistical analysis

Data are presented as mean ± standard error of the mean (SEM), if not stated otherwise. The D'Agostino and Pearson omnibus normality test was used to test for normality. Multiple comparisons were analysed by one-way analysis of variance with Sidak's *post hoc* correction or the Kruskal–Wallis nonparametric test with Dunn's *post hoc* correction. P-values < 0.05 were considered statistically significant. GraphPad Prism (GraphPad Software, La Jolla, CA, USA) was used for data analysis.

RESULTS

PKCβ is the predominant conventional PKC isoform in MPMΦ and its predominance is exaggerated in an HG environment

Since it is known that MPMΦ express PKC [20, 21] and play an important role in PM damage [22, 23], we investigated the mRNA expression of classical PKC isoforms PKCα and PKCβ in MPMΦ isolated from WT mice under NG (10 mM) and different HG conditions. Under basal conditions, PKCβ expression was >50 times higher than that of PKCα (Figure 1A). In a dose-dependent manner, stimulation with glucose led to down-regulation of already low expression of PKCα, while expression of PKCβ was up-regulated, thus exaggerating PKCβ predominance in an HG milieu. Hyperosmolarity effects were excluded by using mannitol controls with equal concentrations. Western blotting demonstrated similar glucose-mediated effects on PKCα/β protein expression (Figure 1B). Although PKCβ mRNA levels were much higher than PKCα, the relative protein isoform abundance seemed to be similar under basal conditions. This apparent discrepancy was due to different sensitivities of antibodies used (Supplementary data, Figure S1A): anti-PKCα antibody was 10-fold more sensitive to its target than anti-PKCβ antibody, resulting in seemingly similar immunoblot intensities (Figure 1B).

As omentum is a significant pool for local proliferation and maturation of MPMΦ [24], we also analysed PKCα/β mRNA expression in omentum of WT mice using an established mouse model for PD [14]. We found similar expression of both PKCα and PKCβ isoforms in saline-treated WT animals. In line with *in vitro* data, only PKCβ was strongly induced in omentum in PDF-treated animals (Figure 1C).

Glucose-treated *PKCβ*$^{-/-}$ MPMΦ are more prone to pro-inflammatory signaling following *in vitro* LPS stimulation

In order to elucidate putative glucose-mediated phenotypical differences between MPMΦ of WT and *PKCβ*$^{-/-}$ mice, cells harvested from respective animals were analysed for anti- (IL-10) and pro-inflammatory (TNF-α, IL-6, MCP-1, MIP-2) mediators both under HG (120 mM) conditions (Figure 1D) and under LPS stimulation (Figure 1E). Compared with WT, *PKCβ*$^{-/-}$ MPMΦ produced significantly lower amounts of TNF-α and IL-10 in control conditions, whereas IL-6, MCP-1 and MIP-2 did not differ significantly. After 24 h in an HG environment, compared with control conditions, the release of both pro-inflammatory mediators as well as anti-inflammatory IL-10 was reduced in WT MPMΦ. No such regulation was present in *PKCβ*$^{-/-}$ cells for IL-6, MCP-1, TNF-α and IL-10, whereas MIP-2 release was significantly up-regulated. Following LPS stimulation for 7 h, WT MPMΦ strongly increased release of both pro-inflammatory cytokines (TNF-α, IL-6, MCP-1 and MIP-2) and anti-inflammatory IL-10. Compared with WT cells, LPS-stimulated *PKCβ*$^{-/-}$ MPMΦ produced significantly more TNF-α, IL-6 and MIP-2 (trend for MCP-1) but failed to increase IL-10 release.

PKCβ deficiency aggravates PDF-induced pro-fibrotic and angiogenic structural damage in the peritoneum and increases deterioration of peritoneal ultrafiltration capacity *in vivo*

The structural and functional effect of PKCβ deficiency during PD was investigated in the *in vivo* mouse model. As evaluated in Masson's trichrome–stained parietal peritoneum, both WT and *PKCβ*$^{-/-}$ animals exposed to standard PDF demonstrated structural peritoneal damage characterized by significant submesothelial thickening due to hypercellularity and deposition of extracellular matrix components, which was much more pronounced in *PKCβ*$^{-/-}$ mice (Figure 2A). Compared with WT, PKCβ deficiency led to a disproportionately high increase of collagen I and III deposition as demonstrated by picrosirius red-staining (Figure 2B). Similarly, the PDF-induced increase of TGF-β was much more pronounced in peritoneal effluents of *PKCβ*$^{-/-}$ mice compared with WT animals (Figure 2C). These structural changes were paralleled by functional changes of peritoneal ultrafiltration. Whereas WT animals showed a significantly marked decrease in ultrafiltration capacity after 5 weeks of PD, *PKCβ*$^{-/-}$ animals completely lost their PM ultrafiltration capacity and even reabsorbed fluid from the peritoneal cavity (Figure 2D).

PDF-induced angiogenic changes in WT animals were mild compared with saline-treated controls but were significantly aggravated in *PKCβ*$^{-/-}$ mice, as evidenced by increased submesothelial CD31 positivity (Figure 3A, B) and VEGF levels in peritoneal effluents (Figure 3C).

PKCβ deficiency increases intraperitoneal cytokine levels *in vivo*

It is already known that animals with an SV129 background have a higher threshold of inflammatory and fibrotic response

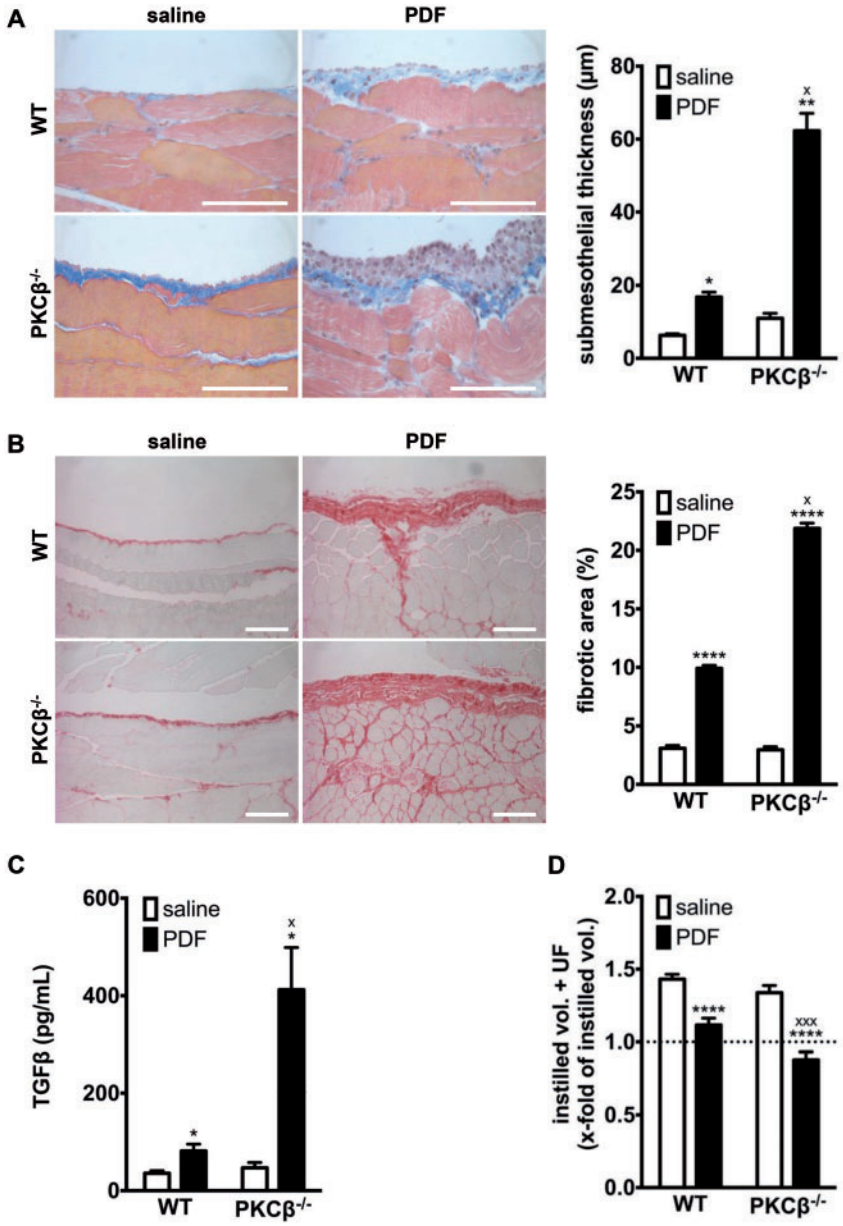

FIGURE 2: PKCβ deficiency exacerbates structural damage to the PM and enhances pro-fibrotic signaling during *in vivo* PD. (**A**) Masson's trichrome staining of the peritoneum and corresponding quantification of submesothelial thickness. PDF-treated WT animals show significant peritoneal thickening of the submesothelial zone, which is much more pronounced in $PKC\beta^{-/-}$ animals ($n = 5$–12 mice/group; $^{*}P < 0.05$ and $^{**}P < 0.01$ versus respective saline group; $^{x}P < 0.05$ versus respective WT group; scale bar = 100 μm). (**B**) Picrosirius red staining of the peritoneum and corresponding quantification of the fibrotic area show that PDF-induced peritoneal fibrosis is exacerbated in PKCβ-deficient animals ($^{****}P < 0.0001$ versus respective saline group; $^{x}P < 0.05$ versus respective WT group; scale bar = 100 μm). (**C**) TGF-β levels in peritoneal effluents obtained on the last day of experiments. Note a disproportionately large increase in TGF-β production among PDF-treated $PKC\beta^{-/-}$ animals ($^{*}P < 0.05$ versus respective saline group; $^{x}P < 0.05$ versus respective WT group). (**D**) Ultrafiltration test shows ultrafiltration failure in both PDF-treated groups and even fluid absorption in the PDF-treated $PKC\beta^{-/-}$ animals ($^{****}P < 0.0001$ versus respective saline group; $^{xxx}P < 0.001$ versus respective WT group).

to glucotoxic challenge in a PD environment than animals with a C57BL/6 background [14]. Thus we were not surprised that PDF-treated and WT animals showed no significant intraperitoneal differences for pro-inflammatory cytokine levels of IL-6, MIP-2, TNF-α and IFN-γ and only a moderate increase of MCP-1 levels in peritoneal effluents. In contrast, $PKC\beta^{-/-}$ animals treated with PDF demonstrated marked increases of these five pro-inflammatory cytokines, both compared with saline-treated $PKC\beta^{-/-}$ mice and compared with PDF-treated WT mice (Figure 4), while concentrations for IL-10, IL-12p70 and IL-17 did not differ significantly (data not shown).

PKCβ deficiency increases inflammatory cell recruitment to the peritoneal cavity

Along those lines, cell influx into the peritoneal cavity in WT mice treated with either saline or PDF did not differ

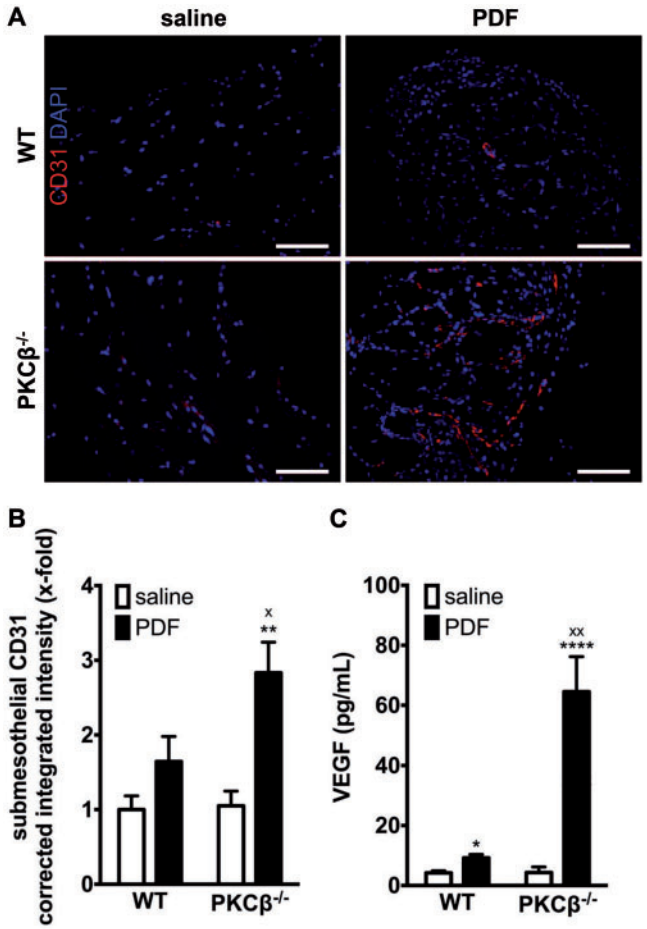

FIGURE 3: PKCβ deficiency aggravates submesothelial angiogenesis and enhances peritoneal VEGF levels during *in vivo* PD. (**A**) Immunofluorescent visualization of $CD31^+$ cells in the peritoneum of WT and $PKC\beta^{-/-}$ animals treated with saline or PDF. Note the increased CD31 positivity in the submesothelial zone of PDF-treated $PKC\beta^{-/-}$ mice (scale bar = 100 µm). (**B**) Quantification of (A), given as background-corrected integrated intensity. Treatment with PDF results in an increased number of $CD31^+$ cells in the submesothelial compartment of the peritoneum in $PKC\beta^{-/-}$ animals (**$P < 0.01$ versus respective saline group; $^{x}P < 0.05$ versus respective WT group). (**C**) Corresponding quantification of VEGF levels by ELISA in peritoneal effluents obtained on the last day of experiments (*$P < 0.05$ and ****$P < 0.0001$ versus respective saline group; $^{xx}P < 0.01$ versus respective WT group).

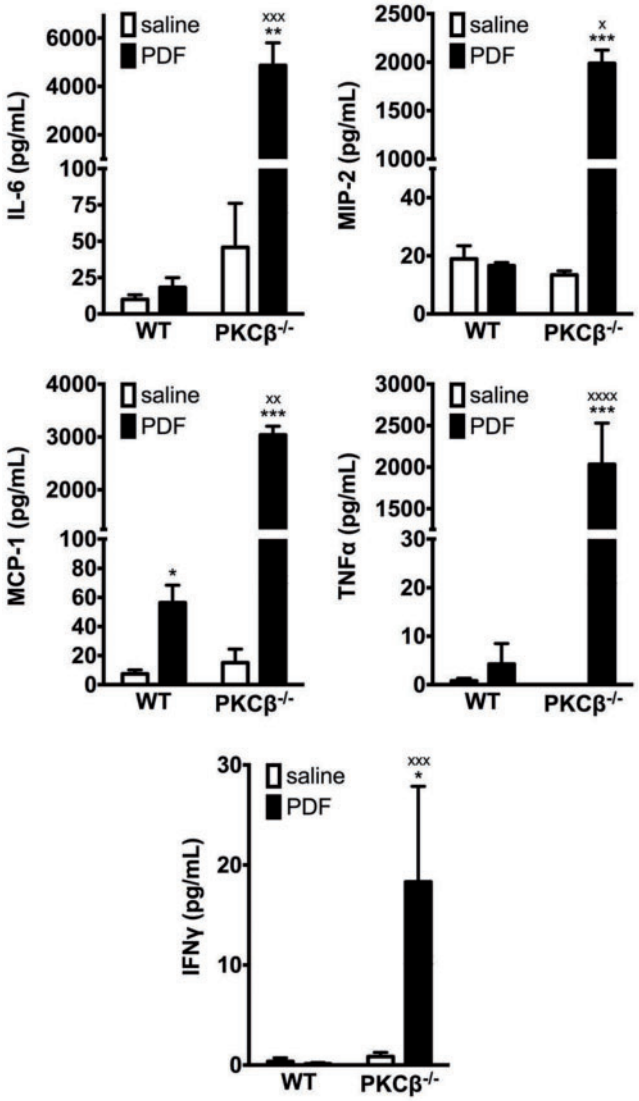

FIGURE 4: PKCβ deficiency markedly increases intraperitoneal cytokine levels. Concentrations of IL-6, MIP-2, MCP-1, TNF-α and IFN-γ in peritoneal effluents. In PDF-treated WT mice only MCP-1 is significantly increased compared with controls. In contrast, concentrations of all five cytokines are strikingly increased in $PKC\beta^{-/-}$ animals undergoing HG-based PD versus saline-treated controls (*$P < 0.05$, **$P < 0.01$ and ***$P < 0.001$ versus respective saline group; $^{x}P < 0.05$, $^{xx}P < 0.01$, $^{xxx}P < 0.001$ and $^{xxxx}P < 0.0001$ versus respective WT group).

(Figure 6). However, we detected a strong accumulation of inflammatory cells on the peritoneal surface in $PKC\beta^{-/-}$ mice exposed to standard PDF, which was not observed in PDF-instilled WT controls (Figure 2A). Mesothelial and submesothelial cell infiltrates visualized by immunofluorescence comprised mainly $F4/80^+$ macrophages, $Gr1^+$ polymorphonuclear (PMN) leucocytes and $CD4^+$ and $CD8^+$ T cells (Figure 5). Correspondingly, flow cytometry identified increased numbers of leucocytes, $F4/80^+$ macrophages, $Gr1^+$ PMN and $TCRb^+$ T cells in peritoneal effluents of $PKC\beta^{-/-}$ animals after PD treatment (Figure 6). B cells of PD-treated $PKC\beta^{-/-}$ animals were neither different compared with WT controls nor compared with saline-treated $PKC\beta^{-/-}$ mice (data not shown).

Infiltrating $F4/80^+$ macrophages in the PM are mainly M1 polarized

Using flow cytometry, we accordingly identified a robust increase of $F4/80^{hi}/MHCII^{hi}$ macrophages, markers consistent with M1 polarization, in peritoneal effluents of PDF-treated $PKC\beta^{-/-}$ animals (Figure 7A), which was not observed in PDF-treated WT mice. Their presence within the PM was confirmed by immunofluorescence: infiltrating $F4/80^+$ macrophages in the mesothelial and submesothelial zone of $PKC\beta^{-/-}$ peritoneum proved to be positive for M1 markers MHCII and CD38 (Figure 7B) and negative for M2 marker arginase-1 (Figure 7C), and thus M1 polarized, which corresponds with disproportionate increases of MCP-1, TNF-α, and IFN-γ in

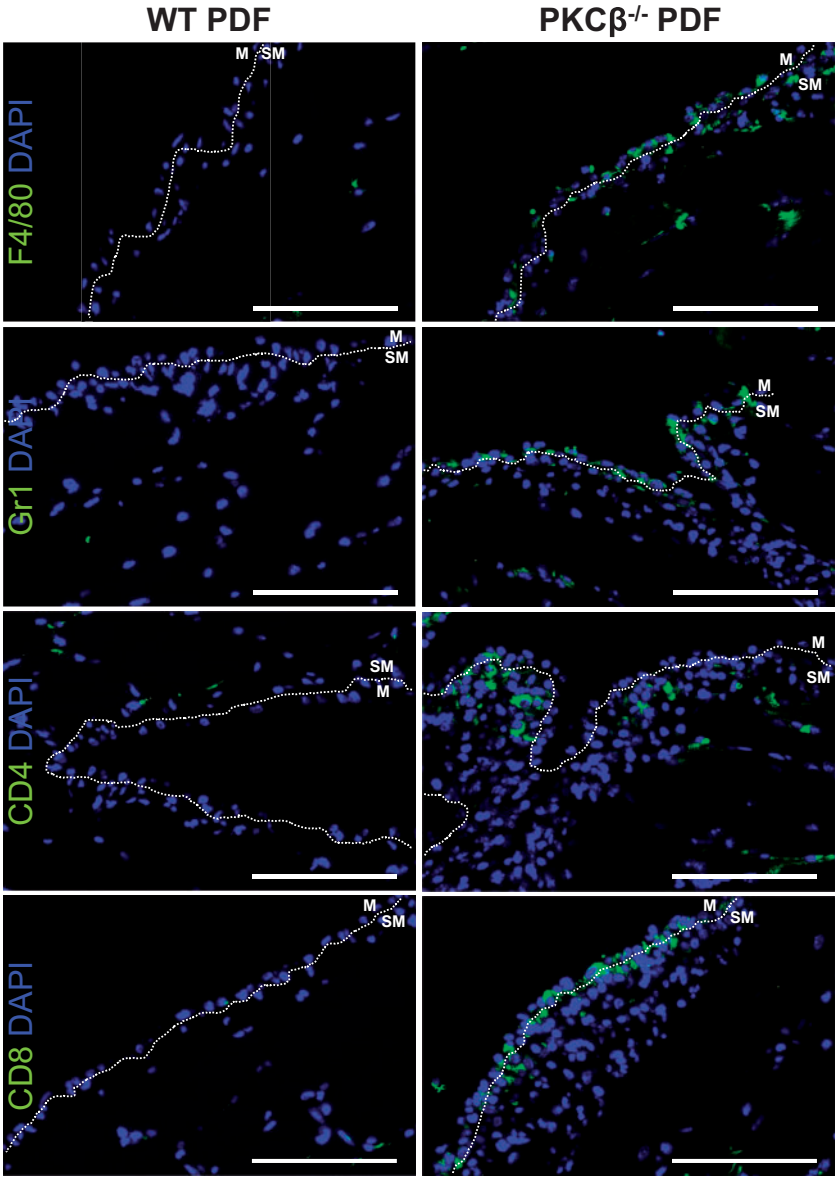

FIGURE 5: PDF-induced mesothelial and submesothelial inflammatory cell influx. Immunofluorescence microscopy analysis of parietal biopsy sections obtained from PDF-instilled mice performed for F4/80$^+$ macrophages, Gr1$^+$ neutrophilic granulocytes (PMN) and CD4$^+$ and CD8$^+$ T cells (scale bar = 100 µm; M, mesothelium; SM, submesothelium).

peritoneal effluents of PDF-treated *PKCβ*$^{-/-}$ animals. In contrast, few infiltrating macrophages in the peritoneum of PDF-treated WT but not *PKCβ*$^{-/-}$ mice showed arginase-1 expression (Figure 7C), indicating an M2 phenotype (MHCII$^-$ and CD38$^-$; Figure 7B).

PKCβ presence is necessary for HG-induced reduction of M1 polarization in PBMC-derived HMΦ *in vitro*

Based on our *in vitro* and *in vivo* data we suggest that PKCβ may also be involved in HG-induced M1/M2 polarization processes in HMΦ. To test this hypothesis, PBMC-derived monocytes were generated from PBMCs of healthy volunteers and differentiated into HMΦ within 7 days before further experimentation in NG or HG conditions. TaqMan analysis revealed that, in contrast to resident MPMΦ (Figure 1A), HMΦ expressed significant amounts of both PKCα and PKCβ isoforms (Figure 8A). However, the expression of PKCβ in HMΦ was higher than that of PKCα and, similar to MPMΦ, stimulation with HG led to up-regulation of PKCβ while expression of PKCα was not changed (Figure 8A). PKCβ siRNA-mediated knockdown was used to block PKCβ expression in HMΦ *in vitro* (Figure 8B, C) prior to incubation under NG (10 mM) or HG (120 mM) conditions for 48 h. To some cells, LPS (100 ng/mL) was added for the last 14 h of incubation. Using flow cytometry, we identified that in NG cultures of different donors ($n = 8$), proportions of CD11b$^+$/HLA-DR$^+$ macrophages (consistent with M1 polarization) varied from 19 to 76% (mean ± SEM 38.06 ± 6.98). However, stimulation with HG significantly decreased both percentages (Figure 8D) and mean fluorescence intensity (MFI, data not shown) of

$CD11b^+$/HLA-DR^+ macrophages in both untransfected (control) and scrambled siRNA-transfected cells. This effect was completely abrogated in cells transfected with PKCβ siRNA (Figure 8D). An additional LPS-induced increase of M1 polarization seen in control and scrambled siRNA-transfected HMΦ incubated in NG was prevented in cells pre-incubated with HG (Figure 8D, E). In contrast, in PKCβ-silenced cells cultured under HG, no effect on M1 polarization was observed after LPS treatment, suggesting an important role of PKCβ in HG/LPS-induced M1/M2 polarization.

Interplay between PKC isoforms: mesothelial PKCα expression is enhanced in human peritoneum of PD patients, in PDF-treated WT mice and further exacerbated in *PKCβ*$^{-/-}$ animals *in vivo*

In patients on PD, PKCα was up-regulated both in the mesothelial and submesothelial layers when compared with non-uraemic control patients (Figure 9A). In addition, we have previously demonstrated that peritoneal PKCα up-regulation is critical for PDF-mediated inflammatory, angiogenic and fibrotic PM damage [14]. Therefore we analysed with immunofluorescence whether PKCβ deficiency would have an effect on PKCα expression. PKCβ deficiency resulted in enhanced mesothelial expression of PKCα under control conditions (saline treatment). As expected, PDF treatment would result in increased PKCα expression, which was further exacerbated in the absence of PKCβ (Figure 9B).

PKCβ deficiency enhances PKCα-driven inflammation under conditions mimicking PD in MPMCs *in vitro* via up-regulation of PKCα expression

Based on this observation, we supposed that up-regulated PKCα expression in *PKCβ*$^{-/-}$ MPMCs may result in enhancement of PKCα-driven PM damage during PD. Therefore, we investigated physiological responses of WT, *PKCα*$^{-/-}$, and *PKCβ*$^{-/-}$ immorto-MPMCs under conditions mimicking PD *in vitro*. MPMCs were cultivated under NG (10 mM) or HG (120 mM) conditions for 24 h and HG-induced MCP-1 release was measured in conditioned medium. As expected, HG treatment of WT cells led to increased MCP-1 release. Whereas this response was completely abrogated in *PKCα*$^{-/-}$ MPMCs, PKCβ deficiency significantly increased MCP-1 release compared with WT cells. To dissect the specific contribution of the respective PKC isoforms, cells stimulated with HG were additionally treated with PKCα/β inhibitor Gö6976, which completely prevented HG-induced MCP-1 release from both WT and *PKCβ*$^{-/-}$ MPMCs but had no additional effect on *PKCα*$^{-/-}$ cells, suggesting a crucial role for the PKCα isozyme (Figure 10A). Along those lines, pharmacological blockade of PKCβ with isoform-specific inhibitor Ly333531 (ruboxistaurin) did not influence MCP-1 production under NG or HG conditions (Supplementary data, Figure S2A).

Western blot analysis revealed that PKCα expression was strongly increased in *PKCβ*$^{-/-}$ compared with WT MPMCs under basal conditions and was further up-regulated after PDF treatment (Figure 10B). As expected, PKCβ protein expression in MPMCs was very low and yielded no signal on western blot

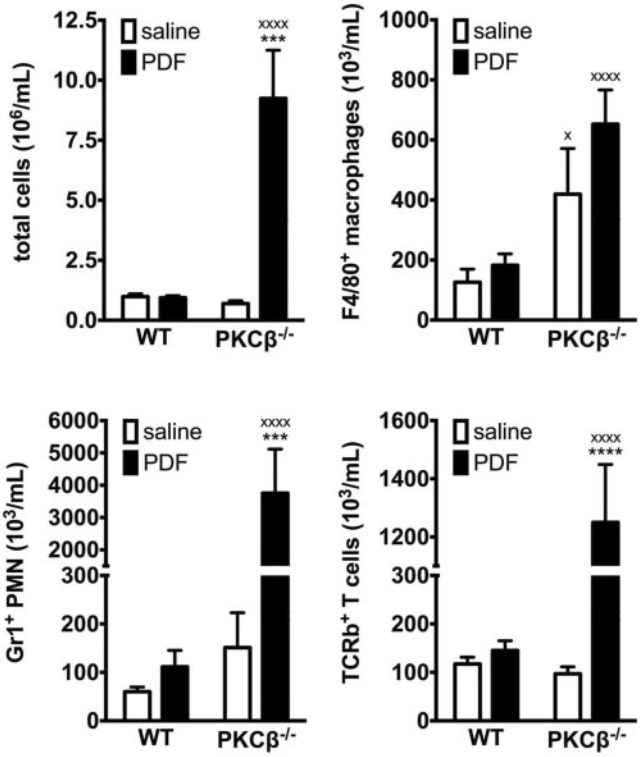

FIGURE 6: PKCβ deficiency dramatically increases inflammatory cell recruitment to the peritoneal cavity. PDF-induced leucocyte influx into the peritoneal cavity assessed by flow cytometry in peritoneal effluents after ultrafiltration testing. Notice that neither PDF treatment in WT animals nor PKCβ deficiency alone affects inflammatory cell influx, whereas PKCβ deficiency in combination with PDF treatment leads to a dramatic increase. Note that F4/80$^+$ macrophages were already significantly increased under basal conditions in *PKCβ*$^{-/-}$ animals (***$P < 0.001$ and ****$P < 0.0001$ versus respective saline group; $^{x}P < 0.05$ and $^{xxxx}P < 0.0001$ versus respective WT group).

(data not shown). Data on PKCα and PKCβ antibody specificity are shown in Supplementary Figure S1B–D. Interestingly, treatment with PKCα/β inhibitor Gö6976 abrogated HG-induced up-regulation of PKCα in *PKCβ*$^{-/-}$ MPMCs (Figure 10B), indicating an involvement of PKCα in its own regulation. Along those lines, we could demonstrate a comparable effect on PKCα mRNA expression levels for MPMCs stimulated with HG for 48 h (Figure 10C). Again, no regulation for already very low levels of PKCβ mRNA expression was present (Figure 10C). As expected, pharmacological blockade of these low PKCβ levels with Ly333531 (ruboxistaurin) had no effect on PKCα mRNA or protein levels (Supplementary data, Figure S2B, C).

Similar effects of PKCβ deficiency were observed both for HG- and LPS-induced inflammatory responses. MPMCs were stimulated with LPS for 24 h (for analysis of MCP-1 and IL-6) and 72 h (for analysis of MIP-2). Whereas LPS stimulation of WT cells led to strong increases of MCP-1, IL-6 and MIP-2 levels in conditioned medium, this response was strongly ameliorated in *PKCα*$^{-/-}$ cells. In contrast, *PKCβ*$^{-/-}$ cells demonstrated massively enhanced cytokine release of all three cytokines in response to LPS stimulation compared with WT

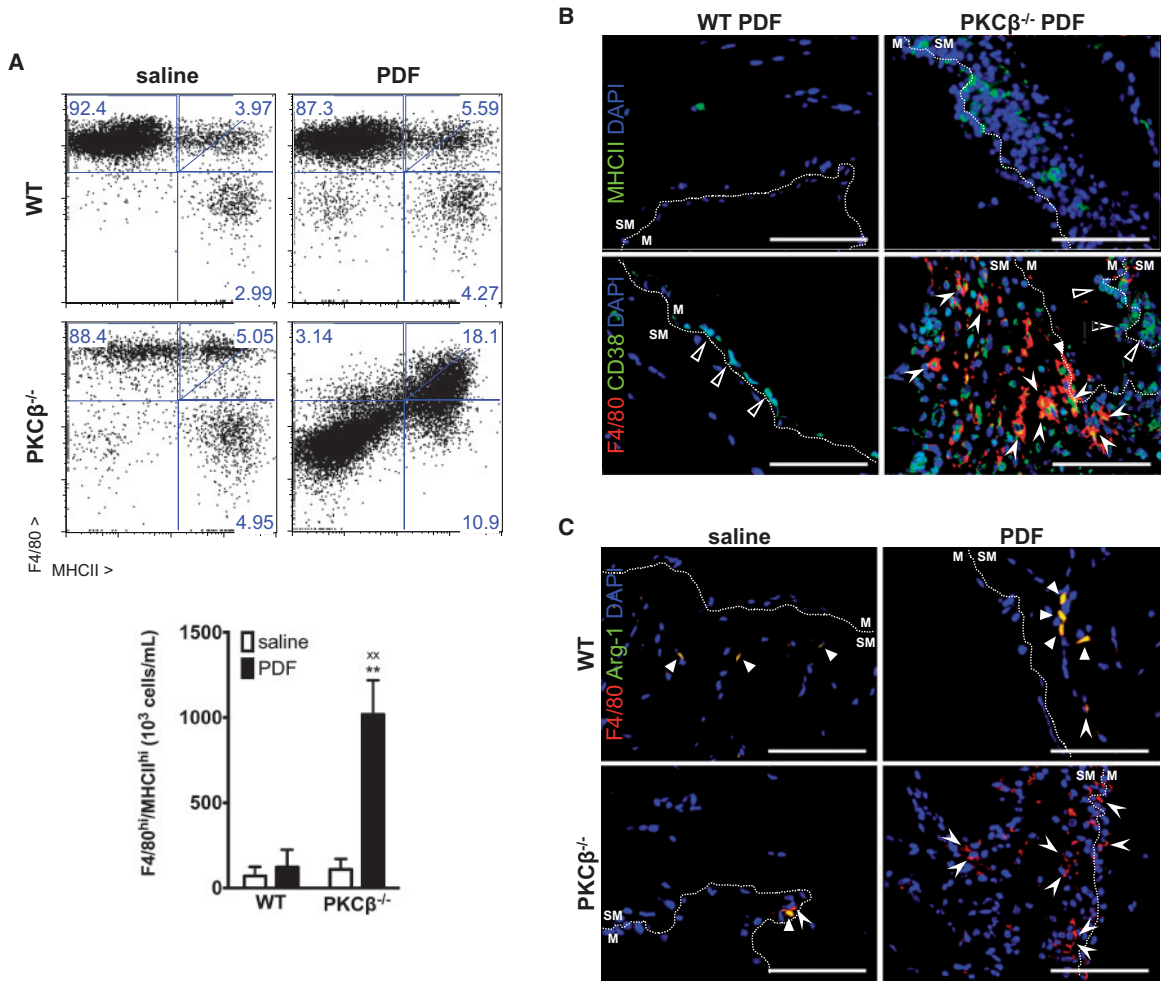

FIGURE 7: Infiltrating F4/80$^+$ macrophages in the PM of *PKCβ*$^{-/-}$ mice are mainly M1 polarized. (**A**) Flow cytometry of peritoneal effluents identified a strong increase of F4/80^{hi}/MHCII^{hi} macrophages in PDF-treated *PKCβ*$^{-/-}$ mice that could not be seen in similarly treated WT animals ($n = 5$–12 mice/group; $^{**}P < 0.01$ versus respective saline group; $^{xx}P < 0.01$ versus respective WT group). (**B**) Immunofluorescent visualization of MHCII$^+$ as well as F4/80$^+$/CD38$^+$ M1-polarized macrophages (arrowheads), F4/80$^+$/CD38$^-$ non-M1-polarized macrophages (solid triangles) and F4/80$^-$/CD38$^+$ cells (empty triangles) in inflammatory infiltrates within the mesothelial layer of the peritoneum (scale bar = 100 μm; M, mesothelium; SM, submesothelium). (**C**) Immunofluorescent visualization of F4/80$^+$/arginase-1$^+$ M2-polarized macrophages (solid triangles) and F4/80$^+$/arginase-1$^-$ macrophages (arrowheads) (scale bar = 100 μm; M, mesothelium; SM, submesothelium).

cells (Figure 10D). In line with our *in vivo* observations, these results demonstrate that pro-inflammatory mediator release in immorto-MPMCs under circumstances mimicking PD is mediated largely by PKCα, the expression of which is in turn negatively regulated by PKCβ.

DISCUSSION

A major limitation of PD is its requirement for glucose as the driving osmotic agent for solute and water exchange across the PM. Chronic glucose exposure, however, is not a genuinely physiological peritoneal process, resulting in changes that have some analogy to glucotoxic effects in diabetes, such as advanced glycation end products accumulation, inflammation, vasculopathy, membrane thickening and extracellular matrix deposition [25].

PKCβ is a classic PKC isoform whose role has not yet been investigated in a peritoneal context. However, involvement of PKCβ in processes relevant for PM damage, such as fibrosis and inflammation, was demonstrated for several models, including diabetes [11], cardiomyopathy [26] and infection [27]. Furthermore, it has been revealed for glucotoxic milieus that PKCα and PKCβ can exert distinct and complementary roles in response to elevated glucose [28].

Using a PD mouse model in *PKCβ*$^{-/-}$ mice compared with WT controls, in this study we demonstrate that PKCβ deficiency results in strongly increased PD-induced inflammation, fibrosis and angiogenesis. Underlying molecular mechanisms involved an M1 polarization shift of MPMΦ and up-regulation of PKCα in MPMCs in *PKCβ*$^{-/-}$ mice.

Resident peritoneal macrophages contribute significantly to chronic inflammation, which is an important determinant of PD complications. Exposure to HG has been shown to induce pro-inflammatory mediator expression in thioglycollate-elicited macrophages [21] and to alter LPS-stimulated macrophage response [29]. Changes in peritoneal macrophage function and activation during PD were demonstrated

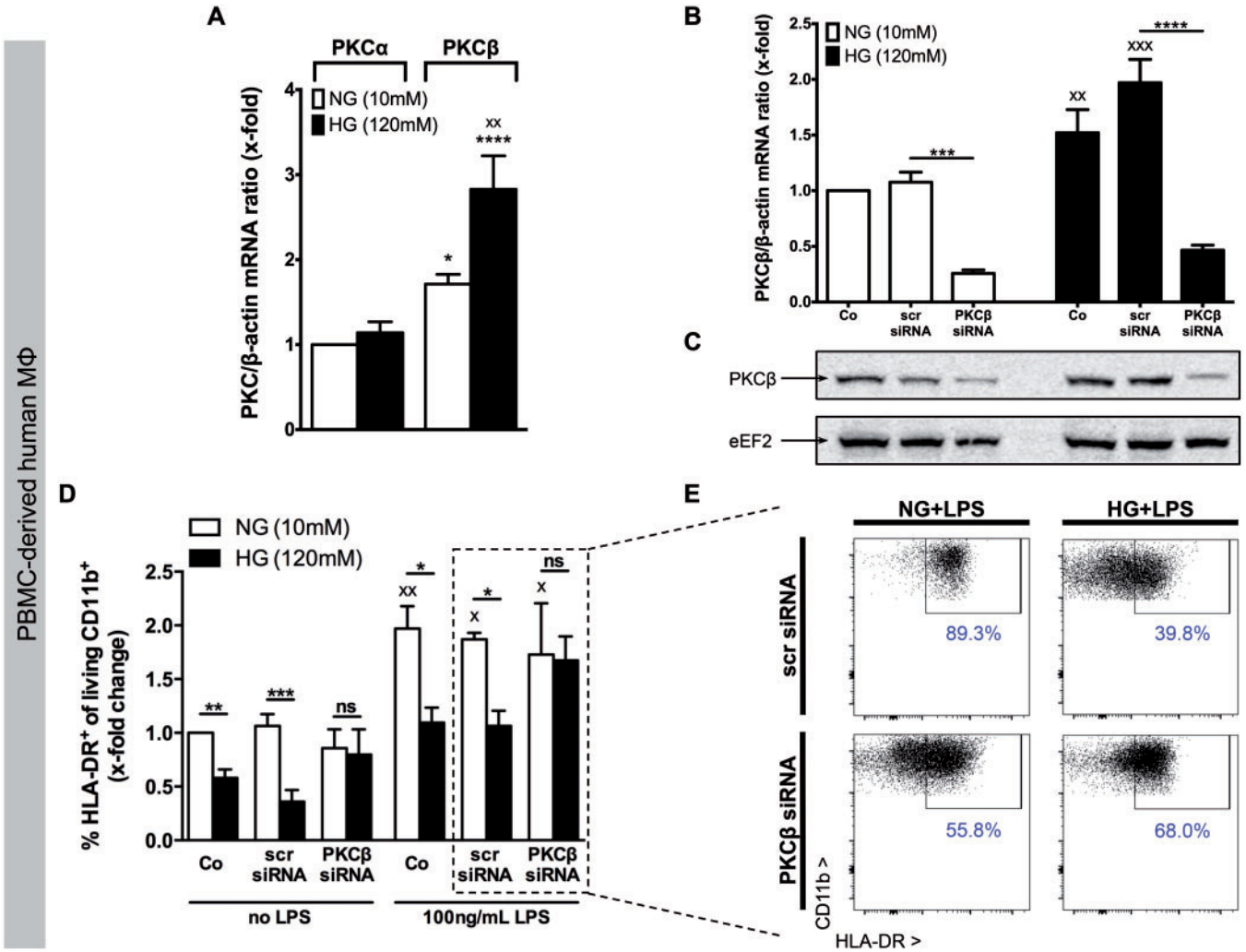

FIGURE 8: PKCβ is involved in HG-dependent HMΦ polarization. (**A**) PKCα and PKCβ mRNA expression of PBMC-derived HMΦ of healthy donors ($n = 8$) evaluated by quantitative real-time PCR. Compared with MPMΦ, HMΦ expressed significant amounts of both PKCα and PKCβ. Predominance of PKCβ over PKCα was exaggerated by HG treatment while PKCα expression remained unchanged (*$P < 0.05$ and ****$P < 0.0001$ versus respective PKCα group; $^{xx}P < 0.01$ versus respective NG group). (**B**) PKCβ-directed siRNA-mediated knockdown in HMΦ cultured in NG and HG conditions was confirmed by real-time PCR (***$P < 0.001$ and ****$P < 0.0001$ versus respective scrambled siRNA group; $^{xx}P < 0.01$ and $^{xxx}P < 0.001$ versus respective NG group; data are representative of eight experiments; scr, scrambled). (**C**) Corresponding representative western blot for PKCβ; cells were treated similarly as in (B). Eukaryotic elongation factor 2 (eEF2) was used as a loading control. (**D**) HG-induced reduction of HLA-DR$^+$ percentage as a marker for M1-polarized HMΦ was abrogated in HMΦ subjected to siRNA-mediated PKCβ knockdown (*$P < 0.05$, **$P < 0.01$ and ***$P < 0.001$ versus respective NG group; $^{x}P < 0.05$ and $^{xx}P < 0.01$ versus respective non-LPS group; data are representative of eight experiments; scr, scrambled). (**E**) Corresponding representative flow cytometry scatterplots of HMΦ treated with scrambled or PKCβ-directed siRNA after LPS stimulation under NG or HG conditions.

>30 years ago [30, 31]. Additionally, recent studies found that in resident peritoneal macrophages, PKC is necessary for fine-tuning inflammatory cytokine responses [16, 21]. The role of specific PKC isoforms, however, remains unclear.

We demonstrate that PKCβ is the predominant classic PKC isoform expressed in primary MPMΦ and its expression is up-regulated *in vitro* under HG conditions, which is in line with previous observations made for human monocyte–derived macrophages [32]. We also demonstrate that HG-reduced pro- and anti-inflammatory mediator release from WT MPMΦ *in vitro* and that PKCβ is necessary for this effect. While data from others have shown up-regulation of pro-inflammatory mediators in response to an HG milieu [21], we attribute these differences to thioglycollate treatment the authors used in order to elicit macrophages to the peritoneum, whereas we analysed resident macrophages as they exist without any activating stimuli prior to HG treatment. In line with these *in vitro* data, prolonged exposure to PDF resulted in PKCβ up-regulation in omentum of WT mice, tissue that is considered a site for local proliferation and maturation of peritoneal macrophages [24].

With the implicit understanding that macrophages exist in complex environments that mostly do not fit traditional M1/M2 polarization categories as extreme endpoints of a continuum, for deduction purposes it is still worthwhile analysing these most extreme states [16]. Data on the interplay of macrophage M1/M2 polarization and PM damage are conflicting:

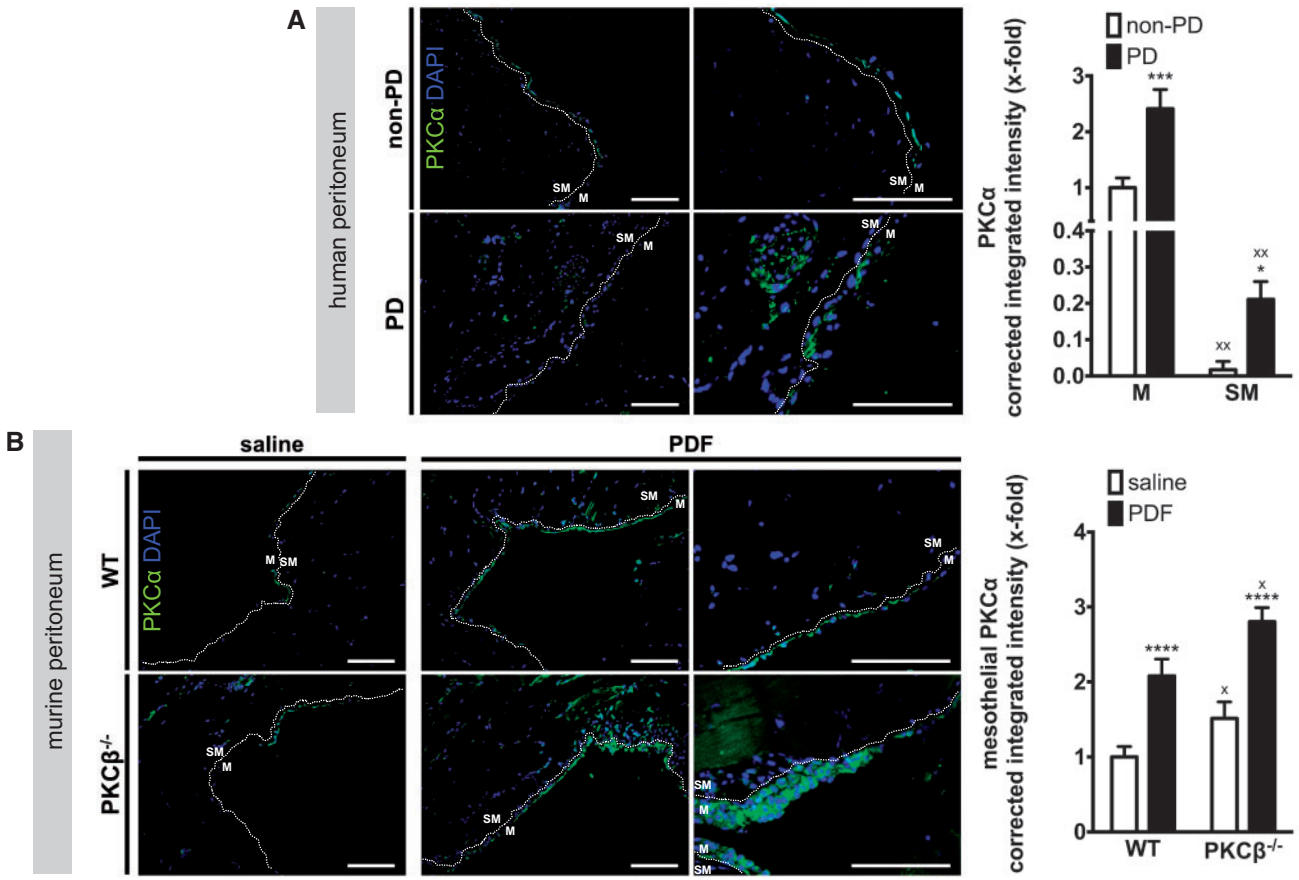

FIGURE 9: PKCα expression in human peritoneum and in the context of genetic presence or deficiency of PKCβ. (**A**) PKCα expression visualized by immunofluorescence in human peritoneal tissue from patients on PD was up-regulated in both the mesothelium and submesothelium compared with non-uraemic patient controls ($n = 2$/group). Quantification was performed on images taken at 20× magnification (*$P < 0.05$ and ***$P < 0.001$ versus respective non-PD group; $^{xx}P < 0.01$ versus respective mesothelial group; scale bar = 100 µm; M, mesothelium; SM, submesothelium). (**B**) PKCα expression visualized by immunofluorescence semi-quantitatively analysed in peritoneal tissues of WT and *PKCβ*$^{-/-}$ animals treated with saline and PDF. PDF-induced up-regulation of PKCα is mainly present in the peritoneum, not in submesothelial compartments, and is more pronounced in *PKCβ*$^{-/-}$ compared with WT animals. Corrected integrated intensity of immunofluorescence for PKCα was quantified for the mesothelial zone in images taken at 20× magnification. Note that control *PKCβ*$^{-/-}$ animals demonstrate higher basal levels of PKCα when compared with WT animals treated similarly with saline (****$P < 0.0001$ versus respective saline group; $^{x}P < 0.05$ versus respective WT group; scale bar = 100 µm; M, mesothelium; SM, submesothelium).

While some reports find either M1 [22, 33, 34] or M2 [35–37] macrophages to be involved in peritoneal fibrosis [34–37], peritonitis [33] and epithelial–mesenchymal transition (EMT) [22], others report both M1 and M2 macrophages to be important for peritoneal fibrosis [38] and encapsulating peritoneal sclerosis development [39]. Along those lines, it is intriguing that the importance of anti-inflammatory IL-10, produced by M2 macrophages, has been recognized as an important parameter determining PD outcome [15, 40–42]. Based on these data and on our *in vitro* results that HG/LPS-stimulated *PKCβ*$^{-/-}$ MPMΦ produced much more pro-inflammatory cytokines but could not produce IL-10, we supposed that the M1 phenotype switch may reinforce a chronic pro-inflammatory environment in *PKCβ*$^{-/-}$ mice. Indeed, we identified that *in vivo* PKCβ deficiency leads to a pronounced shift towards increased M1 polarization, whereas in WT mice mostly M2 macrophages were detected in the peritoneum. The role of PKCβ for macrophage polarization was also confirmed for human cells: an increased proportion of M1-polarized HMΦ was observed after HG stimulation in cells transfected with PKCβ siRNA compared with un-transfected or scrambled siRNA-transfected cells. The M1 shift in *PKCβ*$^{-/-}$ mice was associated with increased inflammation as reflected by strongly increased inflammatory cell recruitment to and cytokine levels within the peritoneal cavity. This inflammatory milieu has direct pro-fibrotic [5] and pro-angiogenic [43] consequences. M1 MPMΦ-derived MCP-1 induces EMT and extracellular matrix synthesis in mesothelial cells via TGF-β up-regulation [44]. TGF-β, in turn, further facilitates peritoneal injury by Smad-dependent and independent pathways [45]. Moreover, direct contact with M1 macrophages has been shown to induce EMT of PMCs [22]. Pro-inflammatory mediators produced by M1 MPMΦ have also been shown to be directly involved in neo-angiogenesis via VEGF induction and modulation of endothelial cell functions [43]. Accordingly, we demonstrate *in vivo* that PKCβ deficiency aggravates PDF-induced PM fibrosis and neo-angiogenesis,

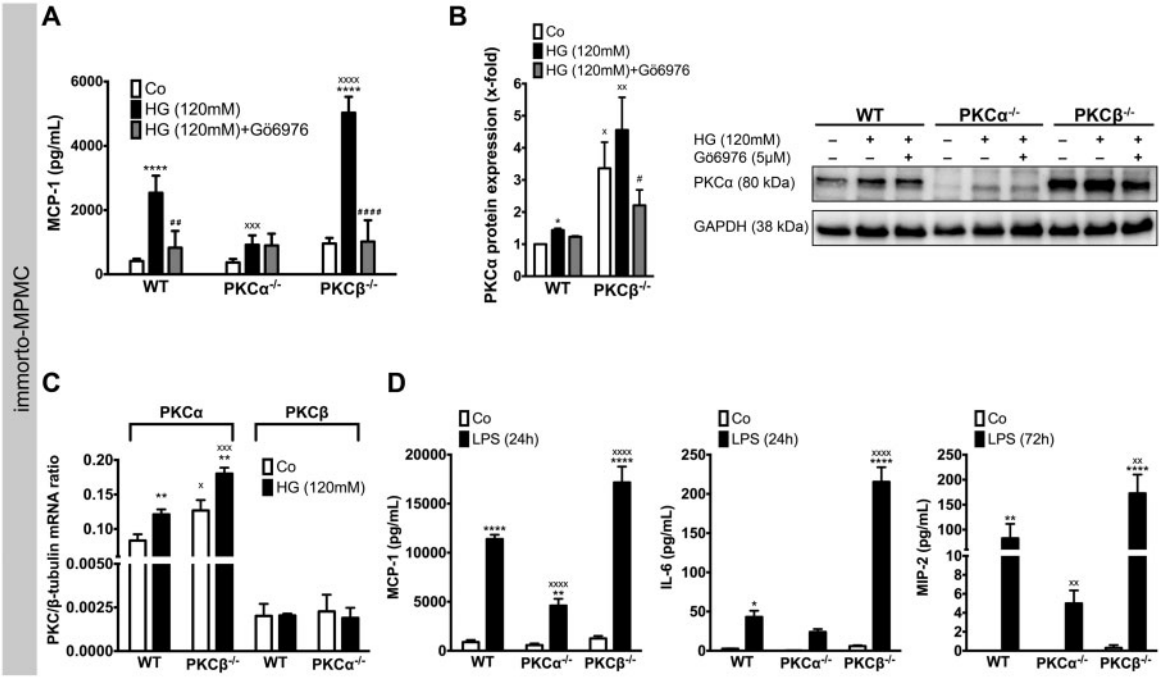

FIGURE 10: PKCβ deficiency markedly increases PKCα-driven inflammation in MPMCs. (**A**) Effect of PKCβ deficiency and pharmacological PKCα/β blockade on HG-induced release of MCP-1 from immortalized MPMCs. Quiescent WT, *PKCβ*$^{-/-}$ and *PKCα*$^{-/-}$ MPMCs were pre-incubated or not for 1 h with 5 μM Gö6976 and thereafter stimulated for 24 h with HG medium. Data are respresentative of three independent experiments performed in duplicates (****$P < 0.0001$ versus respective control (Co) group; $^{\#\#}P < 0.01$ and $^{\#\#\#\#}P < 0.0001$ versus respective HG group; $^{xxx}P < 0.001$ and $^{xxxx}P < 0.0001$ versus respective WT group). (**B**) PKCα protein expression in cell lysates of immortalized MPMCs stimulated as described in (A) analysed by western blotting. Glyceraldehyde-3-phosphate dehydrogenase was used as a loading control. Right panel is representative of three independent experiments quantified in the left panel; quantification of protein expression is given for WT and *PKCβ*$^{-/-}$ MPMCs (*$P < 0.05$ versus respective Co group; $^{\#}P < 0.05$ versus respective HG group; $^{x}P < 0.05$ and $^{xx}P < 0.01$ versus respective WT group). (**C**) Messenger RNA (mRNA) expression levels of PKCα and PKCβ were analysed in MPMCs treated with control conditions as described in (A) or with HG for 48 h. Note that basal up-regulation of PKCα is present in *PKCβ*$^{-/-}$ MPMCs under control conditions with further up-regulation under HG. In contrast, PKCβ mRNA remains unchanged at very low levels. Beta-tubulin was used as a reference (**$P < 0.01$ versus respective Co group; $^{x}P < 0.05$ and $^{xxx}P < 0.001$ versus respective WT group). (**D**) Pro-inflammatory mediator release of MCP-1, IL-6 and MIP-2 was investigated by flow cytometry and specific ELISA, respectively, in immortalized MPMCs stimulated with LPS. Compared with WT cells, LPS-induced mediator release is significantly ameliorated in PKCα-deficient cells, whereas it is significantly enhanced in PKCβ-deficient cells (*$P < 0.05$, **$P < 0.01$ and ****$P < 0.0001$ versus respective Co group; $^{xx}P < 0.01$ and $^{xxxx}P < 0.0001$ versus respective WT group).

paralleled by an exacerbation of TGF-β and VEGF levels in response to HG treatment, which complements data from others showing that PKC isoforms are involved in differential M1/M2 macrophage polarization [46, 47].

We have previously shown that mesothelial PKCα is activated under HG conditions and plays a crucial role in PM pathophysiology mediating inflammatory, neo-angiogenic and fibrotic response [14]. Increased PKCα expression has been demonstrated under inflammatory conditions [48, 49]. Therefore we confirmed that compared with WT controls, the inflammatory milieu in PDF-instilled *PKCβ*$^{-/-}$ mice results in enhanced expression of PKCα. These *in vivo* results are corroborated by *in vitro* findings that immortalized MPMCs stimulated with PDF produce less MCP-1 once PKCα is either genetically absent (in the case of *PKCα*$^{-/-}$ MPMCs) or functionally inhibited (in the case of WT and *PKCβ*$^{-/-}$ MPMCs treated additionally with PKCα/β inhibitor Gö6976). In contrast, MPMCs increase pro-inflammatory mediator release in the case of overexpression of PKCα in PKCβ deficiency. Enhanced PKCα expression in *PKCβ*$^{-/-}$ animals can therefore contribute additionally to PM damage via a positive feedback loop in which inflammation enhances PKCα expression in MPMCs. In turn, PKCα mediates pro-inflammatory mediator release from these cells, facilitating inflammation leading to PM fibrosis and angiogenesis. Interestingly, we found that peritoneal PKCα expression was enhanced in *PKCβ*$^{-/-}$ animals under basal conditions in saline-instilled animals as well as in *PKCβ*$^{-/-}$ MPMCs cultured under NG *in vitro*. These results point to a negative feedback loop between the two classical PKC isoforms PKCα and PKCβ, which corresponds with previous descriptions of feedback inhibition between classical, novel and atypical isoforms [50]. Accordingly, it has recently been shown that genetic deficiency of one PKC isoform has possible knock-on effects on other PKC isoform expression levels [51]. Taken together, we suppose three different mechanisms contributing to increased PKCα expression/activation in MPMCs in *PKCβ*$^{-/-}$ mice: (i) knock-on effects of PKCβ deficiency, (ii) HG-induced up-regulation and (iii) up-regulation within an inflammatory milieu resulting from M1 polarization of MPMΦ.

Our previous findings [14] and the data presented herein strongly support a concept that on both an expression and functional level, PKCα prevails in the mesothelium whereas PKCβ is most important in MPMΦ. Furthermore, we demonstrate that PKCβ both *in vitro* and *in vivo* negatively regulates PKCα on an expression level, that PKCβ deficiency results in pro-inflammatory M1 polarization of MPMΦ and that its presence is therefore necessary to control for mainly PKCα-driven glucose-induced PM damage. Our findings underline the importance of specificity of possible future therapeutic interventions directed at PKC signaling in a peritoneal context.

SUPPLEMENTARY DATA

Supplementary data are available at ndt online.

FUNDING

This research was supported, in part, by grants from the German Research Foundation (Deutsche Forschungsgemeinschaft) to M.S.B. (6205/1-1) and H.H. (1388/17-1). Parts of this manuscript have been presented in abstract form at the ERA-EDTA 2016 Congress and at ASN Kidney Week 2017.

CONFLICT OF INTEREST STATEMENT

None declared.

REFERENCES

1. Kumar VA, Sidell MA, Jones JP *et al.* Survival of propensity matched incident peritoneal and hemodialysis patients in a United States health care system. *Kidney Int* 2014; 86: 1016–1022
2. Yeates K, Zhu N, Vonesh E *et al.* Hemodialysis and peritoneal dialysis are associated with similar outcomes for end-stage renal disease treatment in Canada. *Nephrol Dial Transplant* 2012; 27: 3568–3575
3. Williams JD, Craig KJ, Topley N *et al.* Morphologic changes in the peritoneal membrane of patients with renal disease. *J Am Soc Nephrol* 2002; 13: 470–479
4. Devuyst O, Margetts PJ, Topley N. The pathophysiology of the peritoneal membrane. *J Am Soc Nephrol* 2010; 21: 1077–1085
5. Zhou Q, Bajo MA, Del Peso G *et al.* Preventing peritoneal membrane fibrosis in peritoneal dialysis patients. *Kidney Int* 2016; 90: 515–524
6. Tarafdar A, Michie AM. Protein kinase C in cellular transformation: a valid target for therapy? *Biochem Soc Trans* 2014; 42: 1556–1562
7. Kheifets V, Mochly-Rosen D. Insight into intra- and inter-molecular interactions of PKC: design of specific modulators of kinase function. *Pharmacol Res* 2007; 55: 467–476
8. Liu Y, Jin J, Qiao S *et al.* Inhibition of PKC beta2 overexpression ameliorates myocardial ischaemia/reperfusion injury in diabetic rats via restoring caveolin-3/Akt signaling. *Clin Sci* 2015; 129: 331–344
9. Durpes MC, Morin C, Paquin-Veillet J *et al.* PKC-beta activation inhibits IL-18-binding protein causing endothelial dysfunction and diabetic atherosclerosis. *Cardiovasc Res* 2015; 106: 303–313
10. Batchuluun B, Inoguchi T, Sonoda N *et al.* Metformin and liraglutide ameliorate high glucose-induced oxidative stress via inhibition of PKC-NAD(P)H oxidase pathway in human aortic endothelial cells. *Atherosclerosis* 2014; 232: 156–164
11. Kong L, Shen X, Lin L *et al.* PKCβ promotes vascular inflammation and acceleration of atherosclerosis in diabetic ApoE null mice. *Arterioscler Thromb Vasc Biol* 2013; 33: 1779–1787
12. Park K, Li Q, Rask-Madsen C *et al.* Serine phosphorylation sites on IRS2 activated by angiotensin II and protein kinase C to induce selective insulin resistance in endothelial cells. *Mol Cell Biol* 2013; 33: 3227–3241
13. Menne J, Shushakova N, Bartels J *et al.* Dual inhibition of classical protein kinase C-alpha and protein kinase C-beta isoforms protects against experimental murine diabetic nephropathy. *Diabetes* 2013; 62: 1167–1174
14. Wang L, Balzer MS, Rong S *et al.* Protein kinase C alpha inhibition prevents peritoneal damage in a mouse model of chronic peritoneal exposure to high-glucose dialysate. *Kidney Int* 2016; 89: 1253–1267
15. Liao CT, Andrews R, Wallace LE *et al.* Peritoneal macrophage heterogeneity is associated with different peritoneal dialysis outcomes. *Kidney Int* 2017; 91: 1088–1103
16. Davies LC, Rice CM, Palmieri EM *et al.* Peritoneal tissue-resident macrophages are metabolically poised to engage microbes using tissue-niche fuels. *Nat Commun* 2017; 8: 2074
17. Sherry CL, O'Connor JC, Kramer JM *et al.* Augmented lipopolysaccharide-induced TNF-alpha production by peritoneal macrophages in type 2 diabetic mice is dependent on elevated glucose and requires p38 MAPK. *J Immunol* 2007; 178: 663–670
18. Zhang X, Goncalves R, Mosser DM. The isolation and characterization of murine macrophages. *Curr Protoc Immunol* 2008; Chapter 14: Unit 14.1
19. Ge S, Hertel B, Koltsova EK *et al.* Increased atherosclerotic lesion formation and vascular leukocyte accumulation in renal impairment are mediated by interleukin-17A. *Circ Res* 2013; 113: 965–974
20. Meldrum DR, Meng X, Sheridan BC *et al.* Tissue-specific protein kinase C isoforms differentially mediate macrophage TNFalpha and IL-1beta production. *Shock* 1998; 9: 256–260
21. Wen Y, Gu J, Li SL *et al.* Elevated glucose and diabetes promote interleukin-12 cytokine gene expression in mouse macrophages. *Endocrinology* 2006; 147: 2518–2525
22. Shi J, Li Q, Sheng M *et al.* The role of TLR4 in M1 macrophage-induced epithelial-mesenchymal transition of peritoneal mesothelial cells. *Cell Physiol Biochem* 2016; 40: 1538–1548
23. Sawai A, Ito Y, Mizuno M *et al.* Peritoneal macrophage infiltration is correlated with baseline peritoneal solute transport rate in peritoneal dialysis patients. *Nephrol Dial Transplant* 2011; 26: 2322–2332
24. Van Vugt E, Van Rijthoven EA, Kamperdijk EW *et al.* Omental milky spots in the local immune response in the peritoneal cavity of rats. *Anat Rec* 1996; 244: 235–245
25. Rosenberg ME. Peritoneal dialysis: diabetes of the peritoneal cavity. *J Lab Clin Med* 1999; 134: 103–104
26. Adebiyi OA, Adebiyi OO, Owira PM. Naringin reduces hyperglycemia-induced cardiac fibrosis by relieving oxidative stress. *PLoS One* 2016; 11: e0149890
27. Leitges M, Schmedt C, Guinamard R *et al.* Immunodeficiency in protein kinase Cβ-deficient mice. *Science* 1996; 273: 788–791
28. Jackson R, Brennan S, Fielding P *et al.* Distinct and complementary roles for alpha and beta isoenzymes of PKC in mediating vasoconstrictor responses to acutely elevated glucose. *Br J Pharmacol* 2016; 173: 870–887
29. Hua KF, Wang SH, Dong WC *et al.* High glucose increases nitric oxide generation in lipopolysaccharide-activated macrophages by enhancing activity of protein kinase C-alpha/delta and NF-kappaB. *Inflamm Res* 2012; 61: 1107–1116
30. McGregor SJ, Topley N, Jorres A *et al.* Longitudinal evaluation of peritoneal macrophage function and activation during CAPD: maturity, cytokine synthesis and arachidonic acid metabolism. *Kidney Int* 1996; 49: 525–533
31. Goldstein CS, Bomalaski JS, Zurier RB *et al.* Analysis of peritoneal macrophages in continuous ambulatory peritoneal dialysis patients. *Kidney Int* 1984; 26: 733–740
32. Li L, Sawamura T, Renier G. Glucose enhances human macrophage LOX-1 expression: role for LOX-1 in glucose-induced macrophage foam cell formation. *Circ Res* 2004; 94: 892–901
33. Kang S, Park SJ, Lee AY *et al.* Ginsenoside Rg3 promotes inflammation resolution through M2 macrophage polarization. *J Ginseng Res* 2018; 42: 68–74
34. Li Q, Zheng M, Liu Y *et al.* A pathogenetic role for M1 macrophages in peritoneal dialysis-associated fibrosis. *Mol Immunol* 2018; 94: 131–139
35. Bellon T, Martinez V, Lucendo B *et al.* Alternative activation of macrophages in human peritoneum: implications for peritoneal fibrosis. *Nephrol Dial Transplant* 2011; 26: 2995–3005

36. Wang J, Jiang ZP, Su N *et al.* The role of peritoneal alternatively activated macrophages in the process of peritoneal fibrosis related to peritoneal dialysis. *Int J Mol Sci* 2013; 14: 10369–10382
37. Wang J, Liu J, Wang Y *et al.* High glucose induces alternative activation of macrophages via PI3K/Akt signaling pathway. *J Recept Signal Transduct Res* 2017; 37: 409–415
38. Hu W, Jiang Z, Zhang Y *et al.* Characterization of infiltrating macrophages in high glucose-induced peritoneal fibrosis in rats. *Mol Med Rep* 2012; 6: 93–99
39. Habib SM, Abrahams AC, Korte MR *et al.* CD4-positive T cells and M2 macrophages dominate the peritoneal infiltrate of patients with encapsulating peritoneal sclerosis. *PLoS One* 2015; 10: e0120174
40. Liao CT, Rosas M, Davies LC *et al.* IL-10 differentially controls the infiltration of inflammatory macrophages and antigen-presenting cells during inflammation. *Eur J Immunol* 2016; 46: 2222–2232
41. Min SY, Fu Y, Hutcheson J *et al.* Peritoneal catheter implantation elicits IL-10-producing immune-suppressor macrophages through a MyD88-dependent pathway. *Clin Immunol* 2012; 143: 59–72
42. Onishi A, Akimoto T, Urabe M *et al.* Attenuation of methylglyoxal-induced peritoneal fibrosis: immunomodulation by interleukin-10. *Lab Invest* 2015; 95: 1353–1362
43. Stavenuiter AW, Schilte MN, Ter Wee PM *et al.* Angiogenesis in peritoneal dialysis. *Kidney Blood Press Res* 2011; 34: 245–252
44. Lee SH, Kang HY, Kim KS *et al.* The monocyte chemoattractant protein-1 (MCP-1)/CCR2 system is involved in peritoneal dialysis-related epithelial-mesenchymal transition of peritoneal mesothelial cells. *Lab Invest* 2012; 92: 1698–1711
45. Wong YY, Wong PN, Mak SK *et al.* Persistent sterile peritoneal inflammation after catheter removal for refractory bacterial peritonitis predicts full-blown encapsulating peritoneal sclerosis. *Perit Dial Int* 2013; 33: 507–514
46. Pfeifhofer-Obermair C, Albrecht-Schgoer K, Peer S *et al.* Role of PKCtheta in macrophage-mediated immune response to *Salmonella typhimurium* infection in mice. *Cell Commun Signal* 2016; 14: 14
47. Fan HH, Li L, Zhang YM *et al.* PKCzeta in prostate cancer cells represses the recruitment and M2 polarization of macrophages in the prostate cancer microenvironment. *Tumour Biol* 2017; 39. https://doi.org/10.1177/1010428317701442
48. Zhong C, Wu Y, Chang H *et al.* Effect of PKC inhibitor on experimental autoimmune myocarditis in Lewis rats. *Oncotarget* 2017; 8: 54187–54198
49. Dempsey EC, Cool CD, Littler CM. Lung disease and PKCs. *Pharmacol Res* 2007; 55: 545–559
50. Sudan R, Srivastava N, Pandey SP *et al.* Reciprocal regulation of protein kinase C isoforms results in differential cellular responsiveness. *J Immunol* 2012; 188: 2328–2337
51. Bell KS, Al-Riyami L, Lumb FE *et al.* The role of individual protein kinase C isoforms in mouse mast cell function and their targeting by the immunomodulatory parasitic worm product, ES-62. *Immunol Lett* 2015; 168: 31–40

Received: 7.3.2018; Editorial decision: 2.8.2018

Nephrol Dial Transplant (2019) 34: 960–969
doi: 10.1093/ndt/gfy296
Advance Access publication 15 October 2018

Abundant a proliferation-inducing ligand (APRIL)-producing macrophages contribute to plasma cell accumulation in immunoglobulin G4-related disease

Takahiro Kawakami[1], Ichiro Mizushima[2], Kazunori Yamada[2], Hiroshi Fujii[2], Kiyoaki Ito[2], Tetsuhiko Yasuno[3], Shozo Izui[4], Masakazu Yamagishi[5], Bertrand Huard[6] and Mitsuhiro Kawano[2]

[1]Division of Rheumatology, Department of Cardiovascular and Internal Medicine, Kanazawa University Graduate School of Medicine, Kanazawa, Japan, [2]Division of Rheumatology, Department of Internal Medicine, Kanazawa University Hospital, Kanazawa, Japan, [3]Division of Nephrology and Rheumatology, Department of Internal Medicine, Fukuoka University, Fukuoka, Japan, [4]Department of Pathology and Immunology, University of Geneva, Geneva, Switzerland, [5]Division of Cardiology, Department of Cardiovascular and Internal Medicine, Kanazawa University Graduate School of Medicine, Kanazawa, Japan and [6]Institute for Advanced Biosciences, University Grenoble-Alpes, INSERM U1209, UMR 5309, La Tronche, France

Correspondence and offprint requests to: Mitsuhiro Kawano; E-mail: sk33166@gmail.com

ABSTRACT

Background. This study aimed to investigate the contribution of a proliferation-inducing ligand (APRIL), a member of the tumor necrosis factor (TNF) superfamily implicated in plasma cell survival, to the development of plasma cell–rich lesions in immunoglobulin G4–related disease (IgG4-RD).

Methods. We performed immunohistochemical staining for APRIL with Stalk-1 and Aprily-8 antibodies specifically recognizing APRIL-producing cells and secreted APRIL, respectively, in renal and submandibular lesions of IgG4-RD in comparison with those of Sjögren's syndrome and sialolithiasis.